

## Characteristics of PVA film embedded with Cr<sub>2</sub>O<sub>3</sub> nanoparticles: Optical, electrical, and viscosity

Sakshi Mokashi<sup>1</sup>, Anil Sharma<sup>2</sup>

<sup>1</sup> Research Scholar, Department of Chemistry Kalinga University, Raipur, Chhattisgarh, India

<sup>2</sup> Professor, Department of Chemistry, Kalinga, University, Raipur, Chhattisgarh, India

### Abstract

In order to explore their potential applications in advanced materials, this study examines the optical, electrical, and viscosity properties of polyvinyl alcohol (PVA) films embedded with chromium oxide (Cr<sub>2</sub>O<sub>3</sub>) nanoparticles. In order to assess the impact of different Cr<sub>2</sub>O<sub>3</sub> nanoparticle concentrations on the material's characteristics, PVA films were created using the solution casting method. The optical characteristics were examined using UV-Vis spectroscopy, which showed a marked decrease in optical transmittance with increasing nanoparticle concentration, suggesting increased light absorption. The semiconducting nature of the nanoparticles was attributed to the improvement in electrical conductivity observed with an increase in Cr<sub>2</sub>O<sub>3</sub> content, as measured by means of a four-point probe method. The measurement of the viscosity of the PVA-nanoparticle solution shows that the viscosity increases with the addition of Cr<sub>2</sub>O<sub>3</sub>, indicating that the viscosity is related to the interaction between the nanoparticles and PVA chains. The interaction of the films' optical, electrical, and viscosity properties points to potential uses in sensors, optoelectronic devices, and materials for nanocomposite materials with adjustable characteristics.

**Keywords:** PVA film optical properties, electrical properties, viscosity properties, Cr<sub>2</sub>O<sub>3</sub> nanoparticles

### Introduction

Metal and metal oxide nanoparticles [1, 2, 3] combined polymers have attracted widened application by these hybrid materials [4]. It is well established that certain polymers, as dielectric materials, are excellent host matrices for encapsulation of metal nanoparticles like silver, gold, copper, and so forth, as they act both as reducing as well as capping agents and also provide environmental and chemical stability [5, 6, 7]. At the same time, these embedded nanoparticles inside the polymer matrix also affect the properties of the host itself [8, 9, 10, 11]. Particularly, polymer-metal-nanoparticles composites are promising functional materials in several fields such as optical, electrical, thermal, mechanical, and antimicrobial properties [12, 13, 14, 15, 16]. Many reports in the literature [17, 18] show attempts for synthesis of metal nanoparticles based polymer nanocomposites, with the possibility of variation in their optical and electrical properties for their application in high performance capacitors, conductive inks, and other electronic components. For their application in optoelectronic, electrical, and optical devices, biomedical science, and sensors, main key points are selection of polymer-metal nanoparticles combination, controlling the particles size, their concentration, and distribution within the polymer matrix [19, 20, 21].

In this paper, we have reported the preparation of poly (vinyl alcohol)-Cr<sub>2</sub>O<sub>3</sub> nanocomposites. PVA is water soluble, easily processable, having good film forming and adhesive nature for applications in optical coating and optoelectronic devices. Further, it is also considered as a good host matrix for metal nanoparticles [22]. It is also recognized as one of the very few vinyl polymers soluble in water with a high transparency, excellent thermal stability, chemical resistance, high mechanical strength, moderate, dopant dependent electrical conductivity and good flexibility. A remarkable and advantageous feature of nanoparticles prepared using these techniques in contrast to those

prepared using chemical synthesis is smaller in particle size and absence of uncontrolled by-products [23]. Systematic studies related to the effect of embedding Cr<sub>2</sub>O<sub>3</sub> nanoparticles on the optical and electrical behaviour of the PVA matrix are scarce. A, Hassan *et al.*, has reported the synthesis of nano-sized Cr<sub>2</sub>O<sub>3</sub> by sol-gel method and mixed with PVA to produce nanocomposites films. DSC studies of these films showed the thermal stability and degree of crystallinity of the PVA were reinforced by the addition of Cr<sub>2</sub>O<sub>3</sub> nanoparticles [24]. In this endeavour, we have carried out a systematic study on the effect of embedding of different concentration of Cr<sub>2</sub>O<sub>3</sub> nanoparticles on optical and electrical properties.

### Material and methods

In our lab, we use biological and electrochemical approaches to produce chromium oxide nanoparticles in three distinct ways. After this, films containing nanocomposites of Cr<sub>2</sub>O<sub>3</sub> and PVA were produced.

#### Method 1 (Biological method)

The Mukia Maderaspatana plant extract is combined with the potassium dichromate solution in a beaker and agitated for 10–15 minutes. When the solution's color shifted from orange to green, chromium (III) oxide nanoparticles began to develop.

#### Electrochemical Method 2 (In presence of K<sub>2</sub>Cr<sub>2</sub>O<sub>7</sub> and H<sub>2</sub>SO<sub>4</sub>)

It is possible to electrochemically synthesize chromium oxide nanoparticles using platinum electrodes. See Figure 3.6 for a visual of the experimental setup. A solution of potassium dichromate at 0.3M concentration was settled upon. The components of the electrochemical cell are the platinum electrodes, the voltage source, and the reaction chamber. The experiment included a 20 mL solution of potassium dichromate and a 5 mL solution of concentrated

sulfuric acid (conc. H<sub>2</sub>SO<sub>4</sub>). Positive 12V at 70 mA-90 mA was supplied by the battery eliminator (Neulite India). Three hours passed during which time the experiment was constantly stirred. The color changed dramatically, going from bright orange to emerald green. During two hours at a temperature of 1,000 degrees Celsius, the aforesaid solution was allowed to evaporate slowly. The sulphate test was positive for the dried substance that was collected. In addition, moisture and sulfate as sulfur dioxide were removed by calcining the material at temperatures between 6500C and 7000C.

#### ▪ Electrochemical Method 3 (In the presence of (Pt/Cr) and NaHCO<sub>3</sub>)

The experimental setup is shown in Figure. Electroplating a chromium layer from a chromium nitrate solution onto a platinum electrode (Pt/Cr) was one method used (0.1M). In a reaction chamber, Cr<sub>2</sub>O<sub>3</sub> nanoparticles were synthesized using a 20 ml NaHCO<sub>3</sub> solution. Power was supplied at 12V with 30 mA flowing via a Pt/Cr anode and a Pt cathode. Three hours passed during which time the experiment was done with continual stirring and temperature.

#### PVA-Cr<sub>2</sub>O<sub>3</sub> nanocomposite films preparation

Mixing various quantities of generated Cr<sub>2</sub>O<sub>3</sub> from above-mentioned different processes to PVA solution yields PVA-Cr<sub>2</sub>O<sub>3</sub> nanocomposite films with variable concentrations (0.125%, 0.25%, and 0.5%) of Cr<sub>2</sub>O<sub>3</sub> nanoparticles. This was accomplished by preparing a 1% PVA solution in de-ionized water, adding varying amounts of Cr<sub>2</sub>O<sub>3</sub> while stirring at 500 rpm for an hour to create a uniform viscous solution, and then ultrasonicing the mixture.

### Result and discussion

#### ▪ Optical characterization

Spectrophotometer readings of the UV/Vis absorption spectra are taken between 190 and 1100 nm (Shimadzu-1700 series). Optical absorption spectra for pure PVA and its composites with different amounts of Cr<sub>2</sub>O<sub>3</sub> nanoparticles are shown in Figure. This band is due to the absorption of Cr<sub>2</sub>O<sub>3</sub> nanoparticles into the material. Shifting the nanocomposite films' optical absorption margins from 430 to 360 nm towards the shorter wavelength region [1]. This nanometer-scale blue shift in the optical absorption edge [24] is evidence that Cr<sub>2</sub>O<sub>3</sub> particles are present in the PVA matrix.

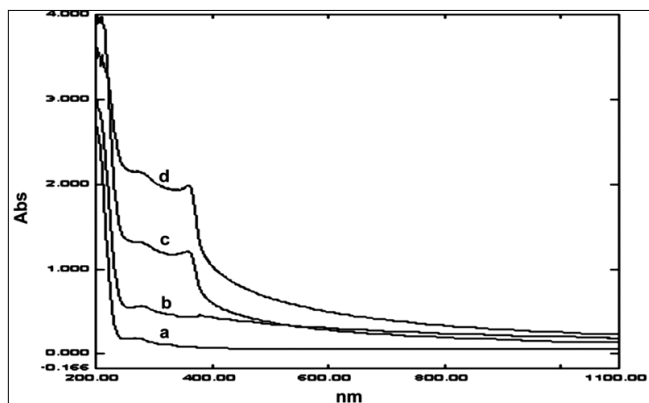


Fig 1: PVA-Cr<sub>2</sub>O<sub>3</sub> nanocomposite film optical absorption spectrum (a) PVA, (b) 0.125% Cr<sub>2</sub>O<sub>3</sub> nanoparticles, (c) 0.25% nanoparticles, and (d) 0.5% nanoparticles

#### ▪ Fourier transform infrared spectroscopy

Absorption spectra are acquired using an ATR (Attenuated total reflectance) instrument attached to a single beam Fourier transform-infrared spectrometer (Bruker Tensor 27-43875). The figure shows 400-4000 cm<sup>-1</sup> FTIR spectra of pure PVA (spectrum a) and PVA-Cr<sub>2</sub>O<sub>3</sub> nanocomposite films (spectrums b-d). In addition, Cr=O vibrational peaks in the range 967-1037 cm<sup>-1</sup>, Cr-O vibrational peaks in the range 585-641 cm<sup>-1</sup>, and Cr-O-Cr vibrational peaks in the range 1046-1085 cm<sup>-1</sup> [1] suggest that Cr<sub>2</sub>O<sub>3</sub> nanoparticles are dispersed throughout the intersites of the PVA polymer matrix. The inclusion of Cr<sub>2</sub>O<sub>3</sub> nanoparticles directly in the PVA film results in a rise in the vibrational intensity of O-H, C-H, and C=O groups in the PVA matrix, as seen in the figure.

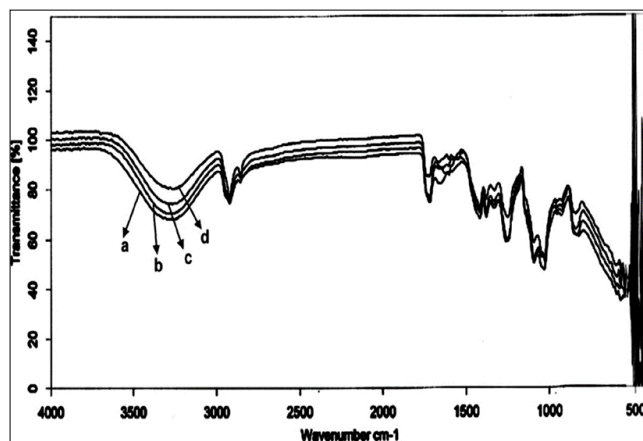


Fig 2: PVA pure film and Cr<sub>2</sub>O<sub>3</sub> nanoparticles doped FTIR spectrum in PVA polymer films in the wavenumber 400-4000 cm<sup>-1</sup>

#### ▪ X-ray diffraction studies

With a Cu k wavelength ( $\lambda$  1.5406) and a scanning range of 00 to 1000, an X-ray diffractometer (Panalytical X-pert) renders crystallographic interpretations. The XRD patterns of pure PVA (curve a) and PVA-Cr<sub>2</sub>O<sub>3</sub> (curves b, c, and d) nanocomposite film at three different Cr<sub>2</sub>O<sub>3</sub> nanoparticle concentrations (0.125%, 0.25%, and 0.5%) are shown in Figure. Figure shows that the relative intensity of this peak decreases after Cr<sub>2</sub>O<sub>3</sub> nanoparticles are embedded in a PVA matrix, and that at 0.5% doping of Cr<sub>2</sub>O<sub>3</sub>, new peaks at 2 $\theta$  values of 24.60, 36.30, 50.20, and 63.60 correspond to the crystal plane of (012), (110), (024), and (214) of crystalline Cr<sub>2</sub>O<sub>3</sub> [1] begin emerging with increased intensities. Characteristic peaks demonstrate that Cr<sub>2</sub>O<sub>3</sub> nanoparticles indeed occur in the amorphous phase of PVA.

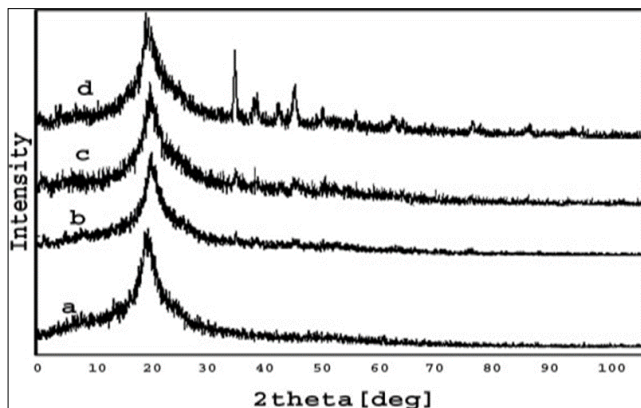


Fig 3: PVA polymer with Cr<sub>2</sub>O<sub>3</sub> nanoparticle doped PVA film X-ray diffraction; (a) PVA, (b) 0.125%, (c) 0.25%, and (d) 0.5%

### Scanning electron microscopy (SEM)

Before and after doping with Cr<sub>2</sub>O<sub>3</sub> nanoparticles at varying filling levels, the surface morphology of polymeric films is examined by scanning electron microscopy (ZESIS). The surface morphology and composition of a

PVA film made using the solution casting method are shown in Figure. SEM images of Cr<sub>2</sub>O<sub>3</sub> nanoparticle-filled PVA films are shown in Figure. All formulations' nanoparticles had roughly spherical forms and exhibited agglomeration.

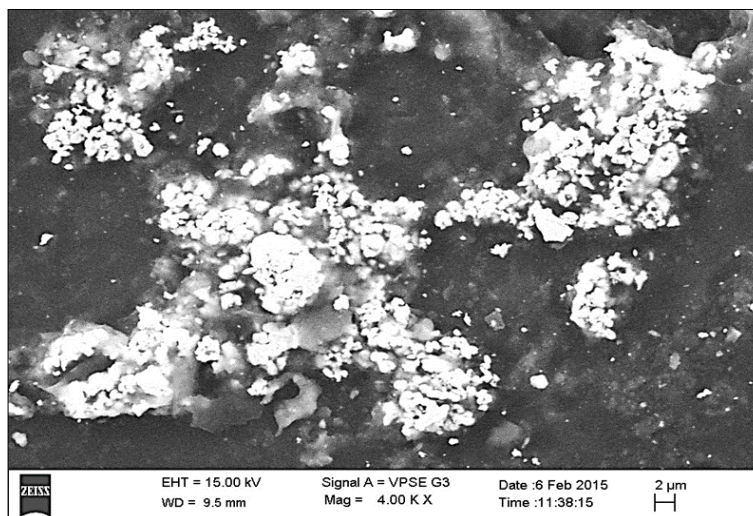


Fig 4: SEM of 0.125% Cr<sub>2</sub>O<sub>3</sub> nanoparticles filled PVA film

### Viscosity measurements

Using an Ostwald viscometer, we measured the solution viscosities of pure PVA and PVA-Cr<sub>2</sub>O<sub>3</sub> nanocomposite at varying concentrations created using three distinct procedures. The Ostwald viscometer is the most common

device of its kind. Care must be taken to ensure that all measurements are conducted with a consistent volume of the solution<sup>[23]</sup> while using this viscometer, which is a basic glass capillary device.

Table 1: Samples of PVA-Cr<sub>2</sub>O<sub>3</sub> nanocomposites were produced at varying Cr<sub>2</sub>O<sub>3</sub> concentrations and their viscosities were measured

Concentration of Cr <sub>2</sub> O <sub>3</sub> C (g/dl)	Concentration Of PVA (g/dl)	Flow time, t (sec)	Relative viscosity $t/t_0 = \eta_r$	Specific viscosity $\eta_r - 1 = \eta_{sp}$	Reduced viscosity $\eta_{sp}/C$ (dl/g)	$\ln \eta_r$	Inherent viscosity $\ln \eta_r / C$ (dl/g)	Intrinsic viscosity $[\eta]$ (dl/g)
0.0119	0.0008	146.17	1.0592	0.0592	74.00	0.0575	71.87	73.25
	0.0012	155.98	1.0892	0.0892	74.33	0.0854	71.16	
	0.0016	166.36	1.1195	0.1195	74.68	0.1128	70.50	
0.0238	0.0008	150.10	1.0876	0.0876	109.50	0.0839	104.87	106.20
	0.0012	162.29	1.1333	0.1333	111.08	0.1251	104.25	
	0.0016	175.41	1.1804	0.1804	112.75	0.1658	103.62	
0.0475	0.0008	155.00	1.1231	0.1231	153.87	0.1160	145.00	147.20
	0.0012	170.14	1.1881	0.1881	156.75	0.1723	143.58	
	0.0016	186.72	1.2565	0.2565	160.31	0.0228	142.68	

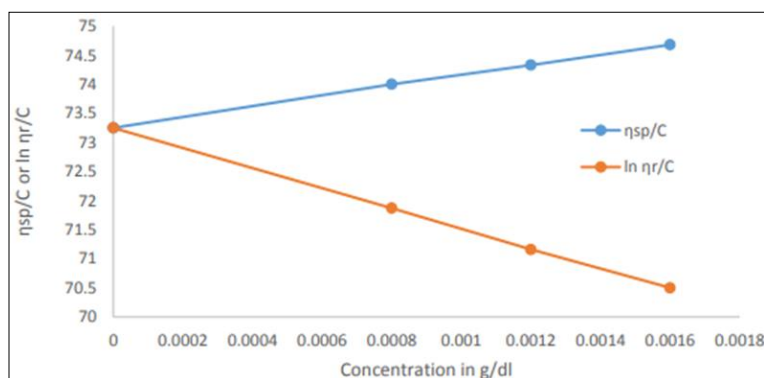
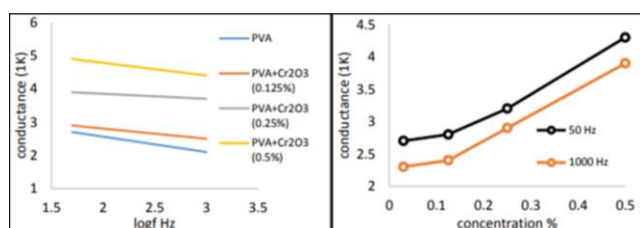


Fig 5: Plots of  $\eta_{sp}/C$  versus  $C$  and  $\ln \eta_r/C$  versus  $C$  for PVA- Cr<sub>2</sub>O<sub>3</sub> nanocomposites samples of method 1 with 0.0119 g/dl of Cr<sub>2</sub>O<sub>3</sub> nanoparticles

### Frequency-dependent conductivity

Using a conductivity bridge instrument, we determine the AC conductivity of PVA and Cr<sub>2</sub>O<sub>3</sub> nanoparticle-embedded PVA films at 50 Hz and 1000 Hz. Figure displays the conductance values at room temperature, and figure displays a plot of conductivity as a function of frequency and concentration for PVA and Cr<sub>2</sub>O<sub>3</sub> nanoparticles implanted PVA films of varied concentrations. Dispersion at low frequencies is shown in AC conductivity, but conductivity falls off sharply with increasing frequency. The electrode-electrolyte contact experiences polarization effects, which cause the low frequency dispersive zone. The non-Debye behavior of the polymer system is shown by a drop in conductivity and an increase in charge buildup at the electrode electrolyte interface with a corresponding drop in the number of mobile ions [22].



**Fig 6:** (a) Plots of AC conductivity versus log f and (b) concentration for PVA and PVA- Cr<sub>2</sub>O<sub>3</sub> nanocomposite films prepared from method 1

### Photo-voltaic activity

Several concentrations of PVA and PVA - Cr<sub>2</sub>O<sub>3</sub> nanocomposite films were tested for conductivity and potential and compared in UV, sunshine, and in the dark. UV-light significantly improves the photovoltaic activity of PVA-Cr<sub>2</sub>O<sub>3</sub> nanocomposite films compared to sunlight and total darkness. UV activity may be explained by the blue shift in the max of Cr<sub>2</sub>O<sub>3</sub> nanoparticles from 430nm to 360nm that occurs upon implantation in a PVA matrix. It may be seen in figure and table.

**Table 2:** Measurement of conductivity and potential of PVA and PVA - Cr<sub>2</sub>O<sub>3</sub> nanocomposite films prepared by three different methods

Property	Sample	U-V	Sunlight	Dark
	PVA	0.05	0.04	0.04
Conductivity measurements in $\mu\text{S}$	PVA+ Cr <sub>2</sub> O <sub>3</sub> (0.125%)	1.47	0.49	0.06
	PVA+ Cr <sub>2</sub> O <sub>3</sub> (0.25%)	1.88	0.52	0.06
	PVA+ Cr <sub>2</sub> O <sub>3</sub> (0.50%)	2.10	0.80	0.07
	PVA+ Cr <sub>2</sub> O <sub>3</sub> (0.125%)	1.54	0.46	0.05
	PVA+ Cr <sub>2</sub> O <sub>3</sub> (0.25%)	1.92	0.49	0.07
	PVA+ Cr <sub>2</sub> O <sub>3</sub> (0.50%)	2.33	0.50	0.05
	PVA+ Cr <sub>2</sub> O <sub>3</sub> (0.125%)	1.45	0.45	0.06
	PVA+ Cr <sub>2</sub> O <sub>3</sub> (0.25%)	2.28	0.50	0.07
	PVA+ Cr <sub>2</sub> O <sub>3</sub> (0.50%)	3.76	0.60	0.04
		PVA	0.014	0.009
Potential Measurements in mV	PVA+ Cr <sub>2</sub> O <sub>3</sub> (0.125%)	0.120	0.010	0.009
	PVA+ Cr <sub>2</sub> O <sub>3</sub> (0.25%)	0.138	0.041	0.007
	PVA+ Cr <sub>2</sub> O <sub>3</sub>	0.157	0.086	0.009
Conductivity Measurements in $\mu\text{S}$	PVA+ Cr <sub>2</sub> O <sub>3</sub> (0.125%)	0.130	0.031	0.009
	PVA+ Cr <sub>2</sub> O <sub>3</sub> (0.25%)	0.141	0.054	0.010
	PVA+ Cr <sub>2</sub> O <sub>3</sub> (0.50%)	0.154	0.090	0.010
	PVA+ Cr <sub>2</sub> O <sub>3</sub> (0.125%)	0.141	0.010	0.011
	PVA+ Cr <sub>2</sub> O <sub>3</sub> (0.25%)	0.158	0.011	0.010
	PVA+ Cr <sub>2</sub> O <sub>3</sub> (0.50%)	0.169	0.012	0.011

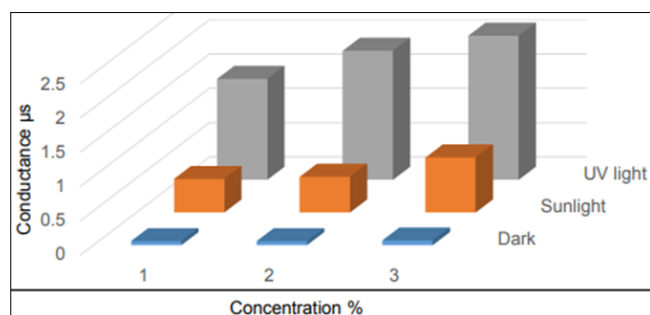


**Fig 7:** Conductivity measurements of PVA- Cr<sub>2</sub>O<sub>3</sub> nanocomposite films of 1.(0.125%) 2. (0.25%) and 3. (0.5%) prepared from method 1

### Conclusion

Three distinct techniques are used to prepare solid polymer films of polyvinyl alcohol (PVA) embedded with varying weight percentages of Cr<sub>2</sub>O<sub>3</sub> nanoparticles using the solution cast technique. Peaks in the FTIR spectra, which are indicative of chemical bonds and molecular vibrations, show that Cr<sub>2</sub>O<sub>3</sub> is present in the PVA polymer structure. Following doping with PVA polymer, the  $\lambda_{\text{max}}$  of Cr<sub>2</sub>O<sub>3</sub> nanoparticles experienced a blue shift, moving from 430 nm to 360 nm. At room temperature, it has been observed that an increase in the concentration of nanoparticles increases the intrinsic viscosity and electrical conductivity of PVA-Cr<sub>2</sub>O<sub>3</sub> nanocomposites.

### References

- Rakesh A S, Netkal M, Made Gowda. Synthesis of Chromium (III) oxide nanoparticles by electrochemical method and mukiamaderaspatana plant extract, characterization, KMNO<sub>4</sub> decomposition and antibacterial study. *Modern Research in Catalysis*,2013;2:127-135.
- Sowbhagya S, Sannaiah A. Synthesis and characterization of se-doped ZnO nanoparticles by electrochemical method: Photodegradation kinetics of indigo carmine dye and study of antimicrobial, antimitotic activities of se-doped ZnO nanoparticles. *American Chemical Science Journal*,2014;4(5):616-637.
- Raksha K R, Sannaiah A, Netkal M, Madegowda. Study of kinetics of photocatalysis, bacterial inactivation and • OH scavenging activity of electrochemically synthesized Se<sup>4+</sup> doped ZnS nanoparticles. *Journal of Molecular Catalysis A: Chemical*,2015;396:319-327.
- Mahshad Ghanipour, Davoud Dorrnanian. Effect of Ag-nanoparticles doped in polyvinyl alcohol on the structural and optical properties of PVA films. *Hindawi Publishing Corporation. Journal of Nanomaterials*, 2013, Article ID 897043.
- Mahendia S, Tomar A K, Kumar S. Electrical conductivity and dielectric spectroscopic studies of PVA-Ag nanocomposite films. *Journal of Alloys and Compounds*,2010;508:406-411.
- Singh N, Khanna P K. In situ synthesis of silver nanoparticles in polymethylmethacrylate. *Materials Chemistry and Physics*,2007;104:367-372.
- Khanna P K, Gokhale R, Subbarao V V V S, Vishwanath A K, Das B K, Satyanarayana C V V. PVA stabilized gold nanoparticles by use of unexplored albeit conventional reducing agent. *Materials Chemistry and Physics*,2005;92:229-233.

8. Akamatsu K, Takei S, Mizuhata M, *et al.* Preparation and characterization of polymer thin films containing silver and silver sulfide nanoparticles. *Thin Solid Films*,2000:359:55-60.
9. Hussain I, Brust M, Papworth A J, Cooper A I. Preparation of acrylate-stabilized gold and silver hydrosols and gold-polymer composite films. *Langmuir*,2003:19:4831-4835.
10. Zavyalov S A, Pivkina A N, Schoonman J. Formation and characterization of metal-polymer nanostructured composites. *Solid State Ionics*,2002:147:415-419.
11. Lee J, Bhattacharyya D, Eastal A J, Metson J B. Properties of nano-ZnO/poly(vinyl alcohol)/poly(ethylene oxide) composite thin films. *Current Applied Physics*,2008:8:42-47.
12. Zhong Z, Wang D, Cui Y, Bockrath M W, Lieber C H. Nanowire crossbar arrays as address decoders for integrated nanosystems. *Science*,2003:302:1377-1379.
13. Hopkins D S, Pekker D, Goldbart P M, Bezryadin A. Quantum interference device made by DNA templating of superconducting nanowires. *Science*,2005:308:1762-1765.
14. Clémenson S, Léonard D, Sage D, David L, Espuche E. Metal nanocomposite films prepared in situ from PVA and silver nitrate. Study of the nanostructuring process and morphology as a function of the in situ routes. *Journal of Polymer Science A*,2008:46:2062-2071.
15. Temgire M K, Joshi S S. Optical and structural studies of silver nanoparticles. *Radiation Physics and Chemistry*,2004:71:1039-1044.
16. Zheng M, Gu M, Jin Y, Jin G. Optical properties of silver-dispersed PVP thin film. *Materials Research Bulletin*,2001:36:853-859.
17. Monti O L A, Fourkas J T, Nesbitt D J. Diffraction-limited photogeneration and characterization of silver nanoparticles. *Journal of Physical Chemistry B*,2004:108:1604-1612.
18. Kelly K L, Coronado E, Zhao L L, Schatz G C. The optical properties of metal nanoparticles: The influence of size, shape, and dielectric environment. *Journal of Physical Chemistry B*,2003:107:668-677.
19. Weickmann H, Tiller J C, Thomann R, Müllhaupt R. Metallized organoclays as new intermediates for aqueous nanohybrid dispersions, nanohybrid catalysts and antimicrobial polymer hybrid nanocomposites. *Macromolecular Materials and Engineering*,2005:290:875-883.
20. Keirbeg U, Vollmer M. *Optical Properties of Metal Clusters*, 25 of Springer Series in Material Science, 1995.
21. Chen S, Sommers J M. Alkanethiolate-protected copper nanoparticles: Spectroscopy, electrochemistry, and solid-state morphological evolution. *Journal of Physical Chemistry B*,2001:105:8816-8820.
22. Suman Mahendia, A K Tomar, Rishi Pal Chahal, Parveen Goyal, Shyam Kumar. Optical and structural properties of PVA films embedded with citrate-stabilized gold nanoparticles. *Journal of Physics D: Appl. Phys.*,2011:44:205105.
23. Rajeev Jain, Nidhi Sharma, Meenakshi Bhargava. *Journal of Scientific and Industrial Research*,2005:63:191-197.
24. Hassen A, El Sayed A M, Morsi W M, El Sayed S. Influence of Cr<sub>2</sub>O<sub>3</sub> nanoparticles on the physical properties of polyvinyl alcohol. *Journal of Applied Physics*, 2012, 112(9).